Photochemistry and Photobiology, Vol. 29, pp. 311–323.

0031-8655/79/0201-0311$02.00/0

PENETRATION OF UV-B AND BIOLOGICALLY EFFECTIVE DOSE-RATES IN NATURAL WATERS*

RAYMOND C. SMITH and KAREN S. BAKER

University of California, San Diego, Scripps Institution of Oceanography, Visibility Laboratory, San Diego, CA 92152, U.S.A.

(*Received* 13 *February* 1978; *accepted* 22 *June* 1978)

Abstract—Spectral irradiance measurements, from 310 to 650 nm, have been made in low and moderately productive ocean waters. These new data and selected earlier clear ocean water data are used as a basis for extrapolating the diffuse attenuation coefficient for irradiance into the 280 nm region. This allows a quantitative calculation of the penetration of UV-B (280-340 nm) and of biologically (DNA) effective dose-rates as a function of depth into various ocean water types. The model of Green *et al.* (1974a) for various atmospheric ozone thicknesses has been used to obtain input surface irradiance for this calculation. Our purpose is to provide a basis for estimating the penetration of possible increased UV-B into natural waters due to possible changes in the ozone concentration of the stratosphere. Given appropriate biological data, this method allows a quantitative evaluation of radiation effects on aquatic organisms as a function of depth. As a specific example, our results have been graphically compared with the dosage-response results on anchovy larvae obtained by Hunter *et al.* (1978).

INTRODUCTION

An increase in the incidence of solar UV radiation upon oceans and lakes, as a consequence of anthropogenic diminishing of the ozone layer in the stratosphere, might well have a significant effect upon primary producers and other organisms in natural waters. In order to make reliable estimates of the potential effects of increased UV radiation incident upon aquatic enviromments, accurate data on the penetration of UV radiation into various types of natural waters are necessary.

Ultraviolet data were obtained as early as 1950 by Jerlov (1950) in a few locations, including the clear waters of the East Mediterranean (reputed to approach the clarity of the Sargasso Sea) and, later, by Lenoble (1955, 1956a, b, c). More recently Calkins (1975) utilized a submersible Robertson–Berger meter to measure the penetration of UV-B into natural waters. These data are limited and have been reviewed by Smith and Tyler (1976) and by Zaneveld (1975).

In order to obtain data necessary for the quantitative evaluation of the biologically effective radiation penetrating into natural waters, a new underwater spectroradiometer has been designed, constructed and data from various water types have been obtained. The maximum penetration of UV-B occurs in ocean waters having minimum concentrations of Chl and dissolved organic material (DOM). Increasing concentrations of these and other dissolved and suspended materials increases the attenuation, and thus decreases the penetration, of UV-B radiation.

*Supported by the United States Department of Commerce, NOAA No. 04-7-158-44039 for the U.S. Environmental Protection Agency, Biological and Climatic Effects Research (BACER) program.

We have placed special emphasis on determining the maximum penetration of UV-B into natural waters by determining the diffuse attenuation coefficient for irradiance, $K(\lambda)$, for clear ocean waters. Only limited data have been obtained for estimating the penetration of UV-B into ocean waters containing more than minimal amounts of Chl *a* and DOM. $K(\lambda)$ data from both low and moderately productive ocean waters have been used, along with Green *et al.*'s (1974a) analytic formulae, to estimate the depth of penetration of UV-B radiation.

With this knowledge of the UV-B radiation, it is possible to calculate biologically effective dose-rates as a function of depth in various natural waters.

DIFFUSE ATTENUATION COEFFICIENT FOR IRRADIANCE

The diffuse attenuation coefficient for irradiance, as distinct from the beam attenuation coefficient, is the appropriate optical parameter to describe the penetration of the sun's radiant energy into natural waters. The distinction between the diffuse and beam attenuation coefficients has been discussed in detail by Tyler and Preisendorfer (1962) and Jerlov (1976). Rationale for the use of the diffuse attenuation coefficient for applications in aquatic biology have been discussed by Smith and Tyler (1976) and applications shown by Smith and Baker (1978a, b).

The total diffuse attenuation coefficient for irradiance, $K_T(\lambda)$, is the optical parameter that relates the spectral irradiance just beneath the ocean surface, $E_d(0^-, \lambda)$, to the downward spectral irradiance at depth Z, viz.

$$E_d(Z, \lambda) = E_d(0^-, \lambda)e^{-K_T(\lambda)\cdot Z}. \quad (1a)$$

The attenuation coefficient is frequently determined experimentally by

$$K_T(Z, \lambda) = \frac{-1}{Z_2 - Z_1} \ln \frac{E_d(Z_2, \lambda)}{E_d(Z_1, \lambda)} \qquad (1b)$$

where $Z_2 > Z_1$ (Z increasing positively downward) are two separate depths at which the downward irradiance has been measured. Note, by inspection of Eq. 1b, that $K_T(\lambda)$ can be determined from a relative measurement of irradiance.

We choose to discuss $K(\lambda)$ for various ocean waters in terms of Chl and dissolved organic material (DOM). From available evidence, Chl (see Smith and Baker, 1978a, b) and DOM (see e.g. Stuemer, 1975; Jerlov, 1976, and references therein) are likely to be among the principal optical components contributing to $K(\lambda)$ in the UV-B region.

Underwater UV-spectroradiometer

Downwelling spectral irradiance was measured using an underwater spectroradiometer which was designed specifically to obtain accurate data in the UV-B portion of the spectrum. This new underwater UV-spectroradiometer was modeled after the original Scripps spectroradiometer (Tyler and Smith, 1966, 1970) but makes use of the latest electrical and optical components. The underwater unit of the new instrument is housed in a pressure case and includes: a Jobin–Yvon double monochromator, a stepping motor and wavelength drive, an EMI 9659 QA photomultiplier, temperature and depth probes, a data acquisition and transmission system, and accessory optics and electronics. The unit has a depth capability of 100 m and is completely remote controlled. A complete description of this instrument is being prepared for publication elsewhere.

For its first deployment at sea, this instrument was used to measure relative (in contrast to absolute) values of spectral irradiance. The only data presented are those for which the wavelength calibration of the instrument at each depth could be checked by comparison with the recognizable spectral structure of the above water spectral irradiance. The above water spectral irradiance, in turn, was calibrated by means of the spectral lines from a mini-mercury lamp. The wavelength calibration for this first deployment at sea may be in error by as much as ± 1 to 2 nm.

K(λ) *for the clearest ocean waters*

The diffuse attenuation coefficient for irradiance is dependent upon and will vary with the optical properties of the dissolved and suspended material in natural waters. Only the clearest ocean waters can be uniquely specified. $K(\lambda)$ measurements from the clearest ocean waters have been reviewed by Smith and Tyler (1976, table 4). These data were used by Smith (1976 unpublished) to form a "best estimate", based on the limited data available, of the diffuse attenuation coefficient for clear ocean waters, $K_W(\lambda)$, in the UV region of the spectrum. This $K_W(\lambda)$ is actually derived from ocean waters where dissolved and suspended material is a minimum (Chl a concentrations of 0.025 mg Chl $a \cdot m^{-3}$ or less). The lowest dashed curve (1) in Fig. 1 is a plot of these data with the dotted portion of the curve representing a best estimate extrapolation of the data.

The new UV-instrument was used for the first time during a cruise in the Gulf of Mexico on the NOAA Research Vessel *Researcher* from 12 October to 30 October 1977. The diffuse attenuation coefficient for irradiance has been derived, by means of Eq. 1b, from measurements of the relative values of downward irradiance. The new UV-spectroradiometer was used to obtain $E_d(Z, \lambda)$ between 310 and 420 nm and the Scripps spectroradiometer was used to obtain data between 360 and 740 nm. The $K(\lambda)$ data from the two instruments agree within experimental error ($\pm 15\%$ for K values below 400 nm) in the spectral region where the data overlaps. A single smooth curve has been drawn through the combined data from 310 to 700 nm.

The clearest water station occupied during our October 1977 cruise was in the middle of the Gulf of Mexico where the Chl a concentrate was 0.05 mg Chl $a \cdot m^{-3}$. Although this is a relatively low Chl (i.e. clear water) value, it is still double that of the waters used for the $K_W(\lambda)$ estimate. The $K(\lambda)$ values obtained at this mid-Gulf station are shown as a solid curve (2) on Fig. 1. They are about 20% higher than the "best estimate" for clearest water $K(\lambda)$ values. This difference is to be expected since there is a measurable difference in the Chl concentrations. The latest measurements lend credibility to the use of the earlier best estimate values of $K_W(\lambda)$ as representing the lowest values for the diffuse attenuation coefficient to be expected in natural waters.

At present we have no reliable data for $K(\lambda)$ values below 310 nm. It should be appreciated, from inspection of Eq. 1b, that the accuracy of $K(\lambda)$ values depends upon the accuracy with which a depth interval ($Z_2 - Z_1$) can be maintained or repeated. From an operational point of view, this depth interval and the minimum near surface depth at which an underwater measurement of spectral irradiance can be obtained are a function of sea state. Further, with shorter wavelengths, the amount of solar radiation is decreasing rapidly while the $K(\lambda)$ function is increasing rapidly giving a very sharp cutoff of radiant energy as a function of wavelength underwater. These factors combined to prevent us from obtaining useful spectral irradiance data below 310 nm on the cruise reported here.

As a consequence $K(\lambda)$ values for this part of the spectral region must be extrapolated from the existing data. We have extrapolated our present $K(\lambda)$ data into this spectral region by "eye" paying attention to the spectral shape and value of our existing $K(\lambda)$ data and to the spectral shape (but not the value) of existing beam attenuation coefficient data below 310 nm. These data are reviewed and discussed by Smith and

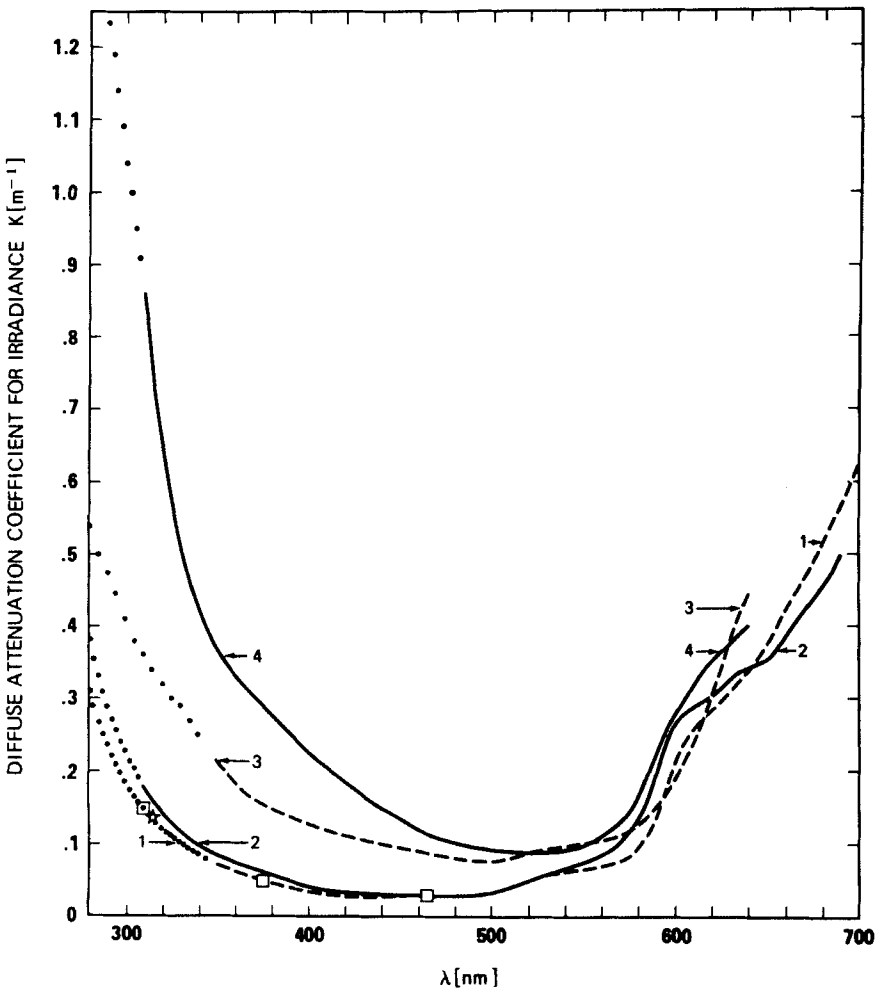

Figure 1. Diffuse attenuation coefficient for downward irradiance, for various water types, as a function of wavelength. *Curve* (*1*) for clearest open ocean waters where productivity is very low (0.025 mg Chl $a \cdot m^{-3}$). The dashed curve is data from the Sargasso Sea (25°43'N 65°41'W) (Tyler *et al.* 1974 as given by Smith and Tyler, 1976, table 4). The individual clear ocean water data points are: □, Jerlov (1950, 1951) Eastern Mediterranean Sea; *, Calkins (1975) clear ocean water near Puerto Rico. The dotted portion of all curves are extrapolations from the actual data. *Curve* (*2*) for clear ocean waters of low productivity (0.05 mg Chl $a \cdot m^{-3}$) from the middle of the Gulf of Mexico (26°00'N, 89°00'W) 22 October 1977. The solid line is data obtained using the underwater UV-spectroradiometer and the Scripps spectroradiometer. The dotted portion of the curve is an extrapolation of this data. *Curve* (*3*) from the model of Smith and Baker (1978b) for moderately productive ocean waters (0.5 mg Chl $a \cdot m^{-3}$). *Curve* (*4*) for moderately productive waters (0.5 mg Chl $a \cdot m^{-3}$) and a relatively high concentration of dissolved organic material from coastal waters northwest of Tampa, FL (28°38.5'N, 83°06.0'W) 15 October 1977. The solid line is data obtained using the underwater UV-spectroradiometer and the Scripps spectroradiometer. Chlorophylls were determined by Baird (1973) for Curve (1) and by Yentsch (private communication) for Curves (2) and (4).

Tyler (1976) who also describe why an estimate of $K(\lambda)$ from beam attenuation coefficient data below 310 nm would be less reliable than the extrapolation given here. The only justification for the present extrapolation is that, given current data, it provides a best estimate of $K(\lambda)$ between 280 and 310 nm.

K(λ) *for ocean waters*

The diffuse attenuation coefficient for irradiance was also measured for moderately productive waters containing larger amounts of Chl and dissolved organic material. A plot of $K(\lambda)$ from a coastal region containing 0.5 mg Chl $a \cdot m^{-3}$ and relatively large amounts of DOM is shown on Fig. 1. The solid curve (4) gives the $K(\lambda)$ values derived from irradiance measurements using the two spectroradiometers and the dotted portion of the curve is our extrapolation of these data below 310 nm.

Also shown on Fig. 1 is a dashed curve (3) for $K(\lambda)$ calculated from the model of Smith and Baker (1978b) for 0.5 mg Chl $a \cdot m^{-3}$. The difference between the top two curves in Fig. 1 can be attributed to the presence of an abnormally high concentration of DOM, relative to Chl *a* plus phaeophytins, in the coastal water region (Yentsch, private communication).

Thus, Fig. 1 presents $K(\lambda)$ curves for four ocean water types: the clearest ocean water containing minimum amounts of Chl a (0.025 mg Chl $a \cdot m^{-3}$) and DOM, waters with very low Chl concentration (0.05 mg Chl $a \cdot m^{-3}$), moderately productive waters (0.5 mg Chl $a \cdot m^{-3}$), and productive waters with this same Chl concentration (0.5 mg Chl $a \cdot m^{-3}$) but containing abnormally high concentrations of dissolved organic material relative to Chl.

PENETRATION OF BIOLOGICALLY EFFECTIVE RADIATION INTO OCEAN WATERS

Global UV-B irradiance

The $K(\lambda)$ data plotted in Fig. 1 have been used to calculate the penetration of biologically effective radiation into ocean waters. Semi-empirical analytic formulae (Green *et al.*, 1974a; Shettle *et al.*, 1974; the computer program for this was provided to us by Green and the parameters used were those he obtained by fitting the semi-empirical model with data from the multiple scattering calculations for a standard atmosphere) for calculating the global UV-B (280–340 nm) reaching the earth's surface have been used to determine the radiation incident on the ocean's surface. Green's formulae accommodate variations in wavelength, solar angle, aerosol thickness, surface albedo and, in particular, ozone thickness, ω_{oz}, so that the possible effects of anthropogenic changes in the ozone thickness can be estimated.

The downward global flux, $E(0^+, \theta, \lambda)$ (which is $G(\theta, \lambda)$ in Green's notation), just above the ocean surface (0^+) is given as the sum of the direct, $E_{sun}(0^+, \theta, \lambda)$, and the diffuse, $E_{diff}(0^+, \theta, \lambda)$, components.

$$E(0^+, \theta, \lambda) = E_{sun}(0^+, \theta, \lambda) + E_{diff}(0^+, \theta, \lambda). \quad (2)$$

In these equations the sun zenith angle θ is calculated from a program which inputs longitude, latitude, date and time. Thus, for a fixed location and date, the above equations may be considered to be a function of the time of day. The total downward irradiance just below the surface (0^-) is calculated by

$$E(0^-, \theta, \lambda) = t(\theta) \cdot E_{sun}(0^+, \theta, \lambda) + t_d \cdot E_{diff}(0^+, \theta, \lambda) \quad (3)$$

where $t(\theta)$ is the transmittance of the air–sea interface as calculated using Fresnell's equations and $t_d = 0.94$ is the transmittance of the air–sea interface for a uniform radiance distribution (Preisendorfer, 1976; Austin, 1974). Having thus calculated $E(0^-, \theta, \lambda)$, the downward spectral irradiance at depth Z is calculated using Eq. 1 and using $K(\lambda)$ values from Fig. 1.

Biological response

The biologically effective irradiance must be based upon a weighting function $\epsilon(\lambda)$ that takes account of the wavelength dependency of biological action. Although the choice of a biological weighting function, $\epsilon(\lambda)$, should be determined by the organism one is studying, a weighting function can be generalized and treated as an approximation for all organisms (Nachtwey, 1975; Setlow, 1974). It is important to realize that the choice of normalizing wavelength for $\epsilon(\lambda)$ is arbitrary. Use of different normalizing wavelengths leads to widely varying values for biologically effective irradiance thus prohibiting significant comparison. However, if $\epsilon(\lambda)$ and its wavelength normalization are specified, then quantitative and significant comparisons can be made between biologically effective dose-rates.

To demonstrate the effect of various water types on the penetration of biologically effective radiation, we have chosen Setlow's DNA action spectrum (Setlow, 1974; as given in analytical form by Green *et al.*, 1975) as representative of a basic action spectra for small ocean organisms. Caldwell's plant response action spectrum (Caldwell, 1971; as given in analytical form by Green *et al.*, 1975), is also used in order to demonstrate the consequences that follow from a different choice of $\epsilon(\lambda)$. In Fig. 2 we have plotted these two $\epsilon(\lambda)$ along with $E(Z, \theta, \lambda)$ for various depths for clearest ocean waters.

As shown by Green *et al.* (1974*b*) the relative biological importance of the various spectral components may be obtained by multiplying the downward irradiance by $\epsilon(\lambda)$ to give the biologically effective dose-rate at each wavelength. Such a result for the downward irradiance, $E_d(0^-, \theta, \lambda)$, and the Setlow DNA action spectrum is shown in Fig. 3. As Green has pointed out, it can be seen that a reduction in ozone concentration has major effects below 310 nm.

Similar curves can be obtained as a function of depth underwater. Figure 4 shows results for the clearest ocean water [curve (1) Fig. 1 and $K(1)$ Table 1] for a "standard atmosphere" ($\omega_{oz} = 0.32$ cm). Several features of these curves can be noted. First, the curve labeled 0^- is the same curve, on a log scale, as the $\omega_{oz} = 0.32$ cm curve in Fig. 3. Second, with increasing depth, the wavelength of the peak response shifts a few nanometers to longer wavelengths. Since some action spectra could show significant wavelength shift in the peak response with depth, it is of interest to note the relatively small shift for the Setlow DNA action spectrum. This is because the sharp spectral drop in DNA response with increasing wavelength is mirrored by an equally sharp drop in the spectral irradiance with decreasing wavelengths (see Fig. 2). Third, most of the integrated area in the semi-log space under these peaks, corresponding to the effective biological dose, lies below 310 nm because of the DNA weighting function. It is important to re-emphasize that the $K(\lambda)$ values below 310 nm are extrapolated from longer wavelengths, as discussed above. Fourth, similar curves for different ω_{oz} values, different latitudes and different times show essentially the same features. The primary difference is the magnitude of the incident response and the position of its wavelength peak.

Figure 5 shows results for our most attenuating example of ocean water [curve (4) Fig. 1 and K(4)

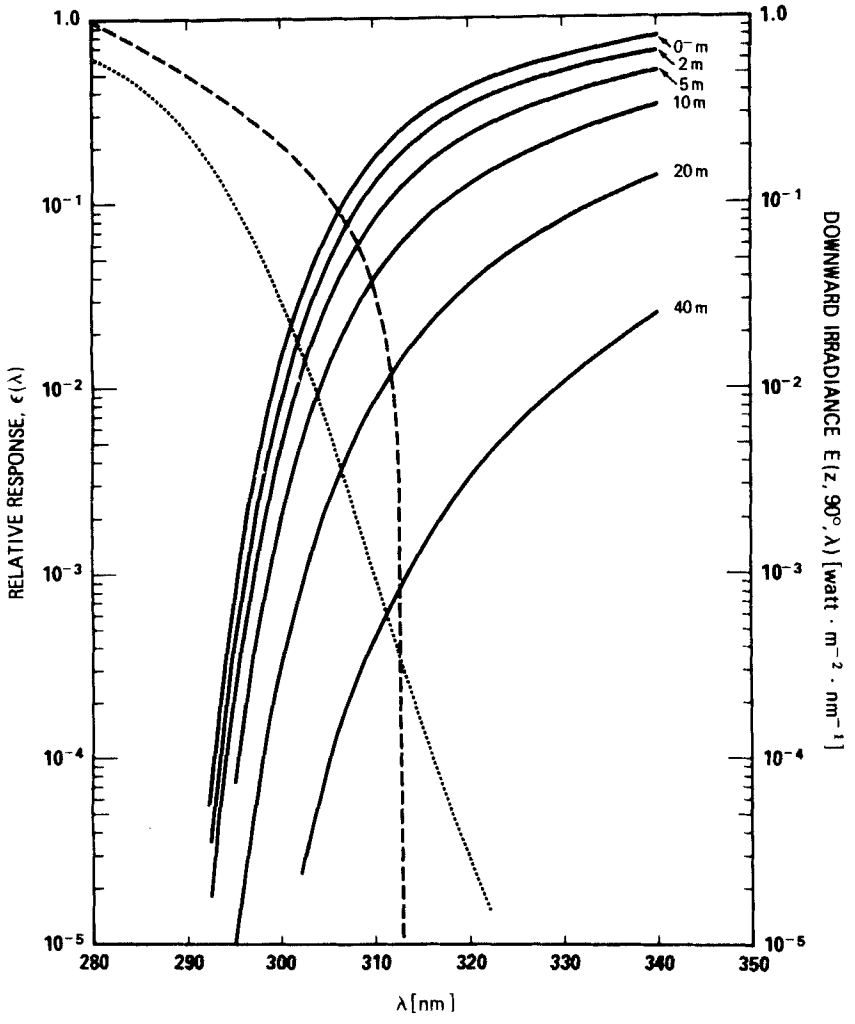

Figure 2. Relative biological efficiencies $\epsilon(\lambda)$ for Setlow's (1974) average action spectrum for biological effects involving DNA (dotted curve) and for Caldwell's (1971) generalized plant response action spectrum (dashed curve) vs wavelength. The relative response (left hand scale) is normalized to 1.0 at the wavelength of maximum response (see Green *et al.*, 1975 for analytical representation). The solid curves (corresponding to the right hand scale) give the downward (noon) spectral irradiance, $E(Z, 90, \lambda)$ $[W \cdot m^{-2} \cdot nm^{-1}]$, at various depths, as a function of wavelength. The product of $\epsilon_{DNA}(\lambda)$ and $E(Z, 90, \lambda)$ gives the curves shown in Fig. 3.

Table 1], again for a standard atmosphere ($\omega_{oz} = 0.32$ cm). The dramatic difference between the curves shown in Fig. 4 and Fig. 5 is the more rapid attenuation of the spectral response with depth of the waters represented in Fig. 5.

Dose

Knowing the relative biological efficiency, or generalized action spectrum, $\epsilon(\lambda)$, for the biological effect under study, one obtains the biologically effective radiation at depth Z by

$$E_B(Z, \lambda)\,[W \cdot m^{-2}]_{\epsilon(\lambda)} = \int E(Z, \theta, \lambda)\,[W \cdot m^{-2} \cdot nm^{-1}] \cdot \epsilon(\lambda) \cdot d\lambda[nm]. \quad (4)$$

We use the notation $[W \cdot m^{-2}]_{\epsilon(\lambda)}$ to indicate a physically measured (or measurable) absolute irradiance weighted by a relative weighting function with an arbitrary normalization wavelength $[\epsilon(\lambda)]$. These units, while arbitrary, are precisely defined and are useful for a comparison with dose-rates in the same units obtained for different situations, e.g. different depths, different ozone thickness, etc. Also, different investigators, having agreed upon a weighting function and wavelength normalization, can quantitatively compare results.

Figure 6 shows the Setlow DNA dose as a function of local time, computed using Green's semi-empirical analytical formulae, for 15 June 1977 at San Diego, CA, for $\omega_{oz} = 0.16$, 0.24, and 0.32 cm. These dosages, for a standard atmosphere, are shown as a function of depth for two water types [$K(1)$ and $K(3)$ of Table 1] in Figs. 7 and 8.

The total daily biologically effective dose at depth Z can be calculated by integrating $E_B(Z, \theta)$ for all

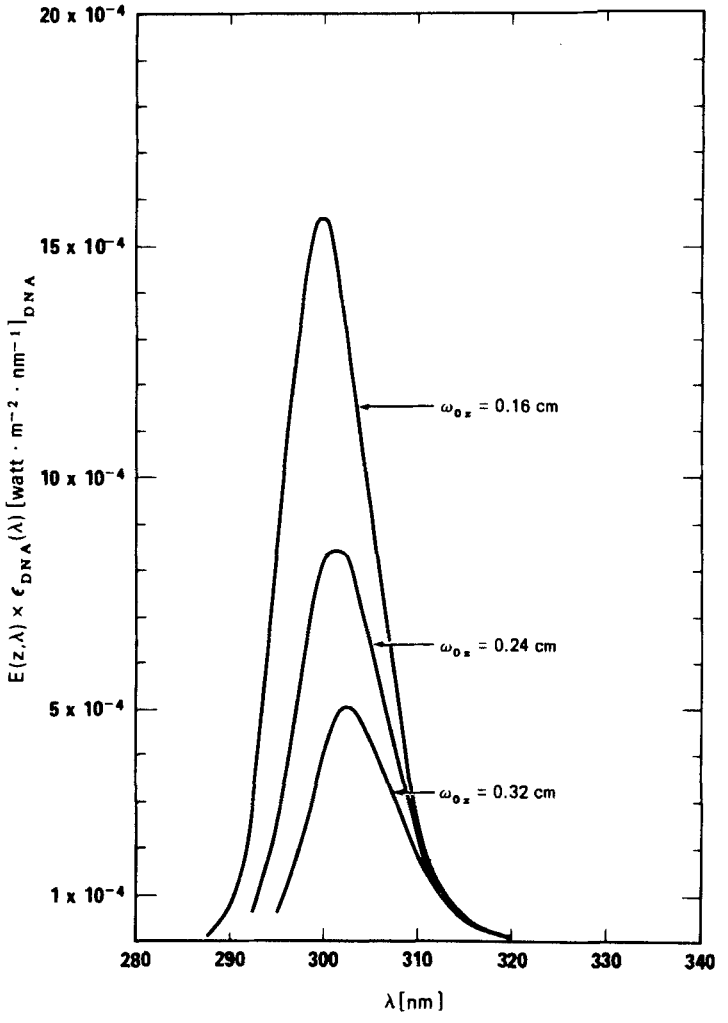

Figure 3. Downward irradiance, $E_d(0^-, \theta, \lambda)$, times the Setlow DNA action spectrum (Setlow, 1974), $\epsilon_{DNA}(\lambda)$, for ozone thicknesses of $\omega_{oz} = 0.16$, 0.24 and 0.32 cm for noon at San Diego, CA (30°N 120°W) on 15 June 1977.

angles over the course of a day, i.e.

$$E_{TB}(Z)[\mathrm{J \cdot m^{-2} \cdot day^{-1}}]_{\epsilon(\lambda)} = \int E_B(Z, \theta)\,[\mathrm{J \cdot s^{-1} \cdot m^{-2}}]_{\epsilon(\lambda)}\,dt[\mathrm{s}]. \quad (5)$$

Thus, given $\epsilon(\lambda)$ and the water's $K(\lambda)$ such as those in Fig. 1 and Table 1, the penetration of biologically effective radiation into various ocean water types can be calculated.

The Setlow DNA weighted dose, for different ozone thicknesses and the four water types given in Table 1, is plotted as a function of depth in Fig. 9. Thus, this figure shows the penetration of biologically effective radiation into various ocean waters. Again, it can be seen that the rate of attenuation of E_{TB} is strongly dependent upon water type.

An interesting feature of the E_{TB} vs Z curves is that they are very nearly straight lines on a logarithmic plot. This follows from the fact, discussed with Figs. 4 and 5, that the wavelength of the response peak changes only a few nanometers with depth. This means the slope of the curves in Fig. 9 may be considered an effective attenuation coefficient for the Setlow DNA action spectrum, K_{DNA}, for the various water types. It should be noted that, for each water type

$$K_{DNA} \approx K(\lambda = 305\,\mathrm{nm}) \quad (6)$$

Thus, a good estimate of the attenuation of biologically effective radiation (for DNA) can be made from a measurement of the diffuse attenuation coefficient at 305 nm.

The curves in Fig. 9, for a given water type, slowly converge. This is understandable since the incident radiation for an ozone depleted atmosphere (say $\omega_{oz} = 0.16$ cm) contains relatively more radiation at low wavelengths, which gives a higher effective attenuation coefficient than that for the standard atmosphere ($\omega_{oz} = 0.32$ cm). This is summarized in Table 2, which lists K_{DNA} for the four water types in Table 1. Three ozone thicknesses and two times of year at the San Diego location are presented. The

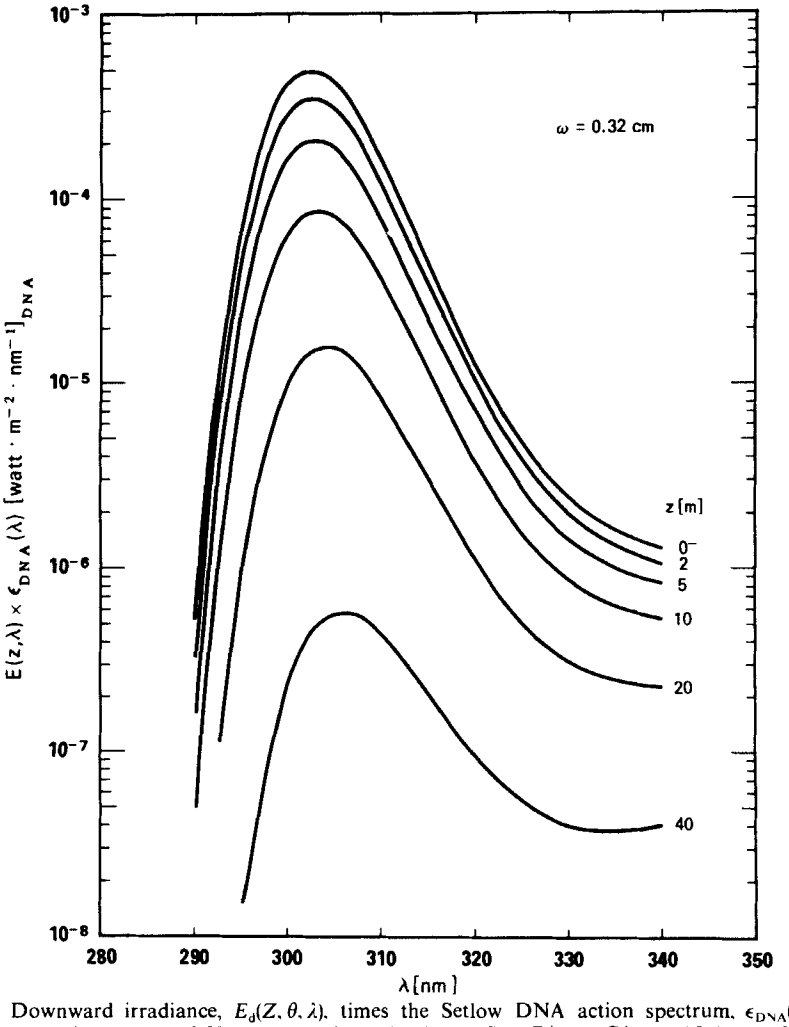

Figure 4. Downward irradiance, $E_d(Z, \theta, \lambda)$, times the Setlow DNA action spectrum, $\epsilon_{DNA}(\lambda)$, for a standard atmosphere (ω_{oz} = 0.32 cm) at various depths at San Diego, CA on 15 June 1977. Data for clear ocean water, Curve (1) in Fig. 1.

Table 1. Diffuse attenuation coefficient for irradiance [m^{-1}]

λ[nm]	K(1)	K(2)	K(3)	K(4)
280	0.310	0.385	0.54	1.43
	0.290	0.355	0.52	1.37
85	0.268	0.332	0.50	1.33
	0.249	0.310	0.49	1.29
290	0.237	0.290	0.47_5	1.24
	0.223	0.271	0.46	1.19
95	0.209	0.256	0.44_5	1.15
	0.198	0.243	0.42_5	1.09
300	0.186	0.228	0.41	1.05
	0.175	0.214	0.39_5	1.00
05	0.166	0.204	0.38	0.96
	0.157	0.192	0.37	0.91
310	0.150	0.180	0.36	0.86
	0.142	0.170	0.35	0.81
15	0.136	0.162	0.34	0.76
	0.129	0.153	0.33	0.72
320	0.122	0.146	0.32	0.68
	0.117	0.139	0.31	0.63
25	0.113	0.132	0.30	0.60
	0.107	0.126	0.29_5	0.56
330	0.103	0.120	0.29	0.53
	0.098	0.115	0.28	0.50
35	0.094	0.110	0.27	0.47
	0.090	0.106	0.26	0.45
340	0.087	0.102	0.25	0.42

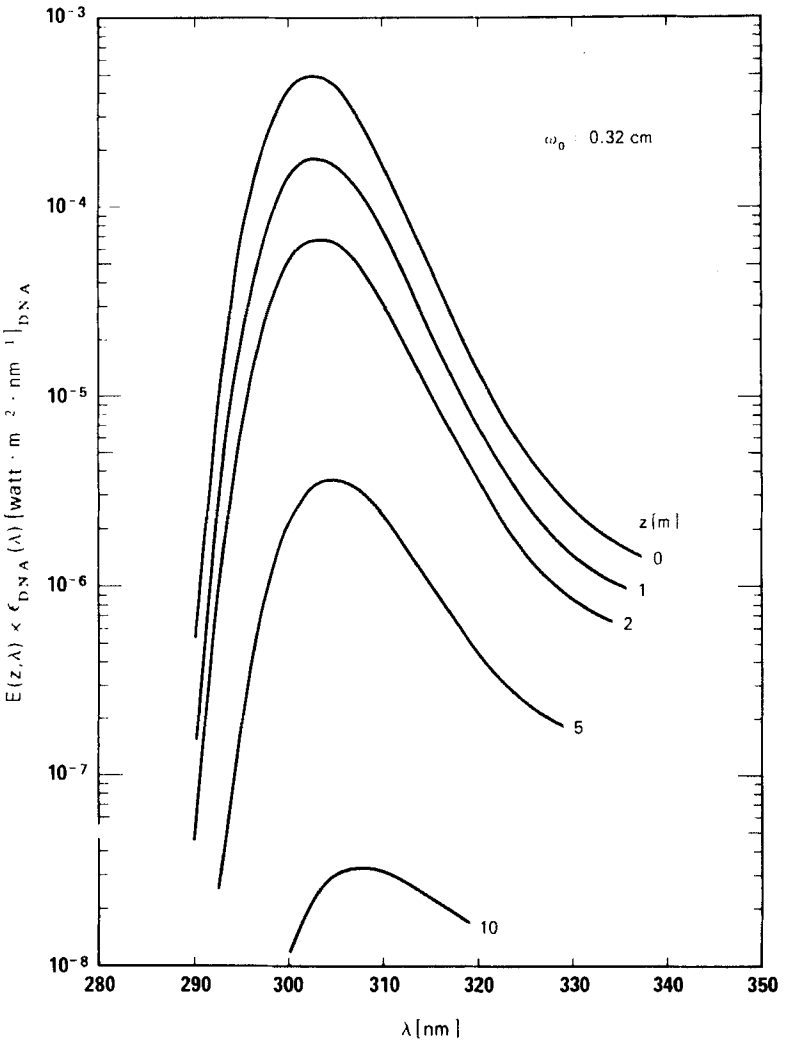

Figure 5. $E_d(Z, \theta, \lambda) \cdot \epsilon_{DNA}(\lambda)$ vs λ for $\omega_{0z} = 0.32$ cm at various depths at San Diego on 15 June 1977. Data for moderately productive coastal water with relatively high concentration of dissolved organic material, Curve (4) in Fig. 1.

winter K_{DNA} values are slightly lower than the summer values because there is relatively less UV-B in winter which leads to an effective attenuation coefficient that corresponds to slightly longer wavelengths.

The choice of a particular $\epsilon(\lambda)$ and its wavelength normalization not only influences the calculated value of the effective dose-rate, it also affects the calculated attenuation with depth into natural waters. The diffuse attenuation coefficient, $K(\lambda)$, increases with decreasing wavelength in the UV region. Therefore, those weighting functions that emphasize the contribution of shorter wavelengths to effective dose-rate will have higher K values, leading to a particular relative effective dose-rate occurring at a shallower depth than would be the case when using a weighting function that emphasizes the contribution at longer wavelengths. This can be seen by comparing Figs. 9 and 10 or Tables 2 and 3. The total daily dose, weighted according to Caldwell's generalized plant response action spectrum, is plotted as a function of depth for three ozone thicknesses in Fig. 10.

Several features on Figs. 9 and 10 should be noted. First, a reminder that the weighting functions were normalized at different wavelengths which means the plant and DNA total daily doses cannot be compared on an absolute basis. Second, the effective attenuation for a plant response dose is less than that for DNA, but only slightly so. Third, if by decreasing the ozone layer the surface dose is increased by $X\%$, then the dosage at all depths is increased by approximately $X\%$ (it would be exactly $X\%$ if it were not for the slight shift in effective K values). It is important to recognize that if the dose at the surface is doubled, then the dose at all depths will also be doubled.

Underwater doses to eggs and larvae of the northern anchovy

We have presented data on the optical properties of water in the UV-B region in order to provide a basis for estimating the penetration of possible increased UV-B into natural waters. As a specific example, the following presents a collaborative calcu-

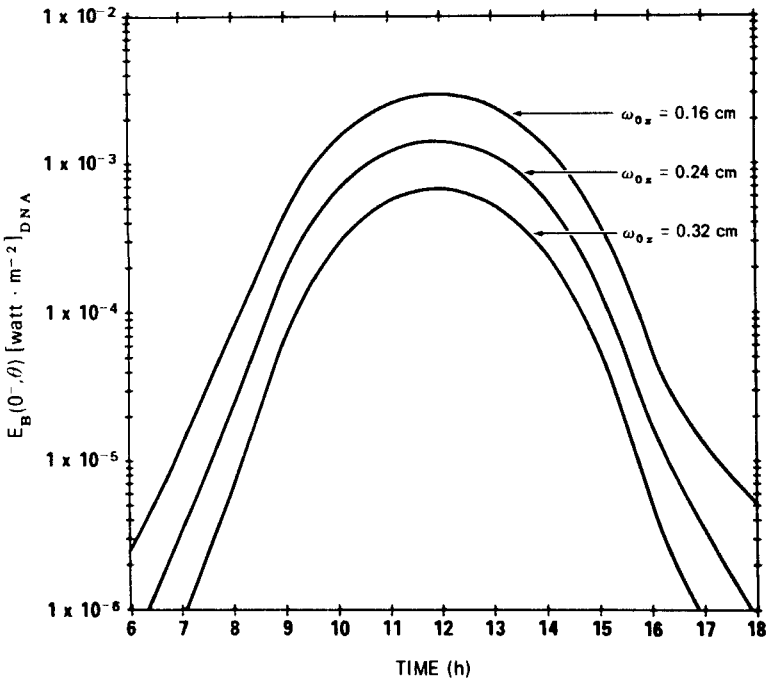

Figure 6. Dose, $E_B(0^-, \lambda)$ $[W \cdot m^{-2}]_{DNA}$ (Setlow DNA action spectrum weighted), as a function of local time computed using Green's semi-empirical analytical formulae (Green *et al.*, 1974a) for 15 June 1977 at San Diego, CA (30°N, 120°W) for ω_{oz} = 0.16, 0.24 and 0.32 cm.

lation applicable to the work of Hunter *et al.* (1978). In order to make our calculations consistent with Hunter's experimental methods, we have calculated a 4 day DNA weighted dose, for different ozone thicknesses, by again using the semi-empirical analytic formulae of Green *et al.* (1974a).

Hunter *et al.* (1978), in studying the effects of UV-B on the eggs and larvae of northern anchovy, found that the Setlow DNA action spectrum was the best available choice of biological weighting function to fit their data. Thus, our above results, obtained as described using Eqs. 1 to 5 and plotted in Fig. 9,

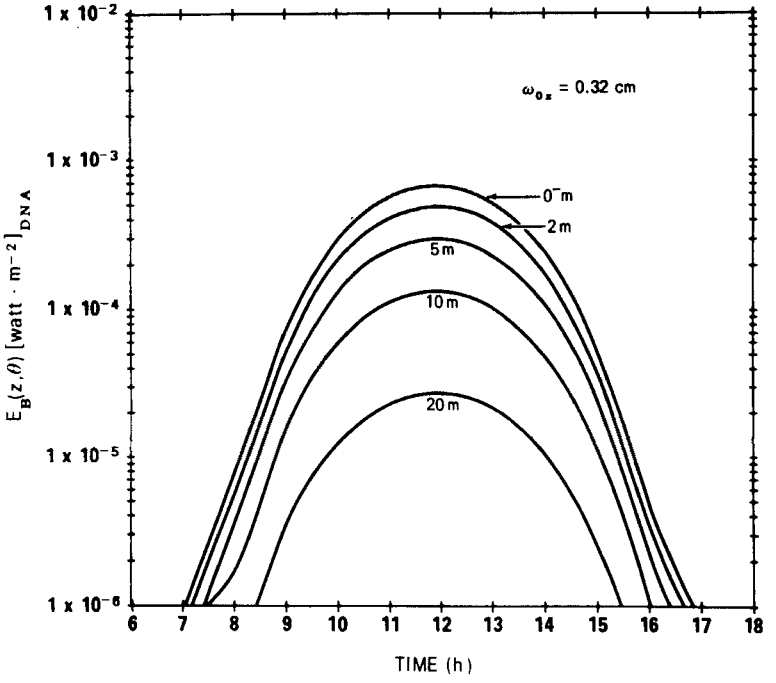

Figure 7. $E_B(Z, \theta)$ $[W \cdot m^{-2}]_{DNA}$ vs local time for 15 June 1977 at San Diego for ω_{oz} = 0.32 cm at various depths in clear ocean water [Curve (1) in Fig. 1]. These data correspond to the data shown in Fig. 4.

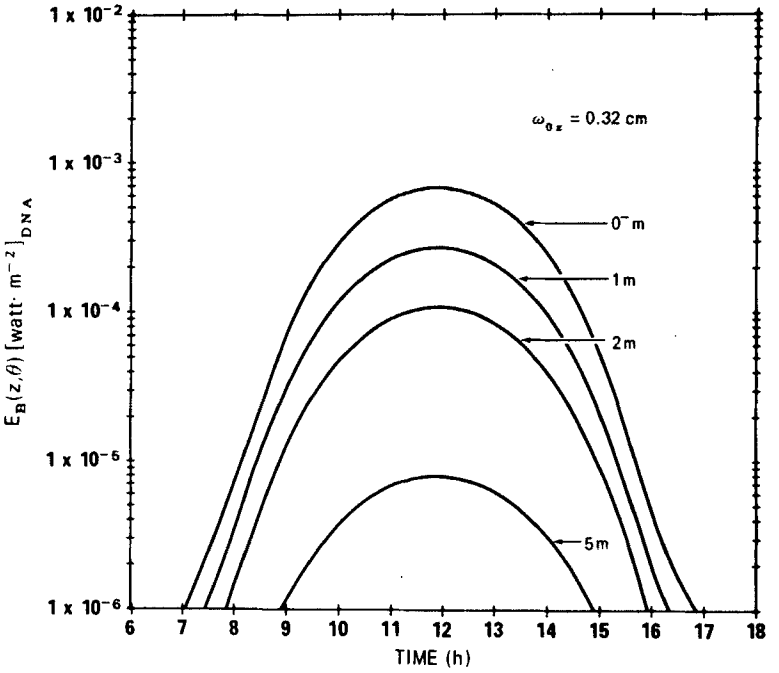

Figure 8. $E_B(Z,\theta)$ [W·m^{-2}]$_{DNA}$ vs local time for 15 June 1977 at San Diego for ω_{oz} = 0.32 cm at various depths in moderately productive high DOM ocean water [Curve (4) in Fig. 1]. These data correspond to the data shown in Fig. 5.

are applicable to Hunter's data. For direct comparison we have plotted our results in Fig. 11 along with those of Hunter.

The solid curves [$K(1)$ in Table 1] in Fig. 11 correspond to the clearest ocean water and give the maximum expected penetration of UV-B (DNA weighted) radiation; the dotted dashed curves [$K(2)$] are for low productivity waters (0.05 mg Chl a·m^{-3}); the

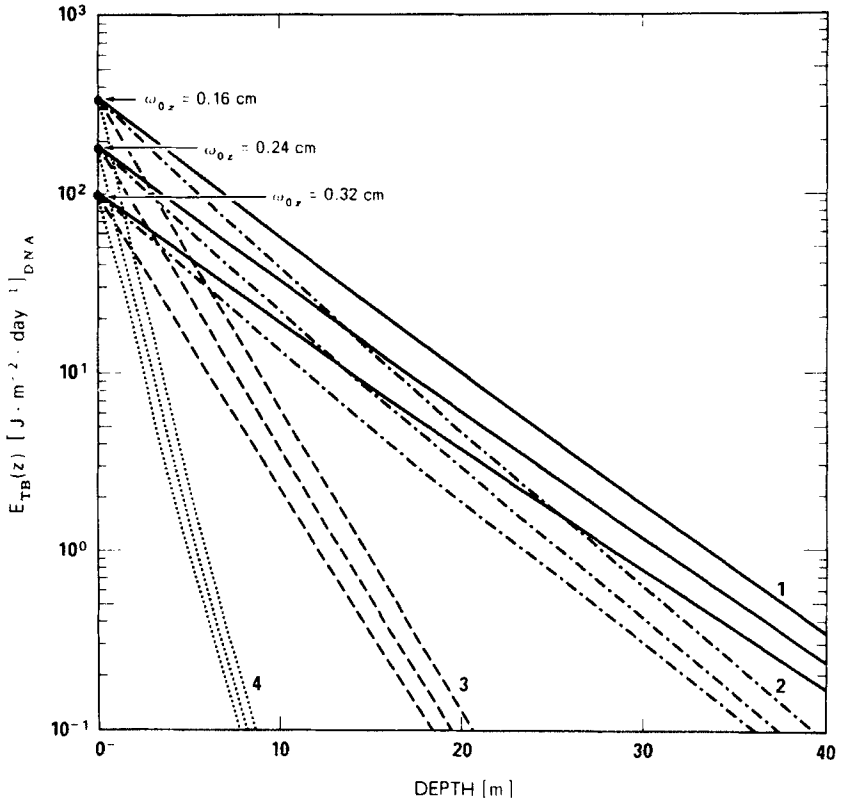

Figure 9. Total daily dose, $E_{TB}(Z)$ [J·m^{-2}·day^{-1}]$_{DNA}$ (Setlow DNA action spectrum weighted), vs depth [m] for various water types and ozone thicknesses (ω_{oz}). The solid curves are for water type labeled (1) in Fig. 1 [and K(1) in Table 1], the —·— curves for water type labeled (2), the – – – curves for water type labeled (3), and the ···· curves for water type labeled (4).

Table 2. Effective attenuation coefficient for irradiance weighted by the Setlow DNA action spectrum, $K_{DNA}[m^{-1}]$

K_{TYPE}	ω_{oz}[cm]	15 June $K_{DNA}[m^{-1}]$	15 December $K_{DNA}[m^{-1}]$
1	0.16	0.176	0.171
	0.24	0.167	0.163
	0.32	0.163	0.155
2	0.16	0.215	0.209
	0.24	0.204	0.198
	0.32	0.197	0.186
3	0.16	0.400	0.394
	0.24	0.384	0.384
	0.32	0.377	0.371
4	0.16	1.00	0.98
	0.24	0.96	0.94
	0.32	0.92	0.87

Table 3. Effective attenuation coefficient for irradiance weighted by the Caldwell generalized plant response action spectrum, $K_{PLANT}[m^{-1}]$

K_{TYPE}	ω_{oz}[cm]	15 June $K_{PLANT}[m^{-1}]$	15 December $K_{PLANT}[m^{-1}]$
1	0.16	0.166	0.162
	0.24	0.162	0.159
	0.32	0.161	0.156
2	0.16	0.200	0.196
	0.24	0.197	0.192
	0.32	0.195	0.190
3	0.16	0.384	0.378
	0.24	0.381	0.375
	0.32	0.378	0.372
4	0.16	0.94	0.92
	0.24	0.92	0.90
	0.32	0.90	0.89

dashed curves [$K(3)$] correspond to our estimated K_{DNA} for moderately productive ocean waters (0.5 mg Chl $a \cdot m^{-3}$) with "normal" concentrations of dissolved organic material and the dotted curves [$K(4)$] refer to this same moderately productive water with "abnormally high" concentrations of DOM relative to Chl *a*.

Hunter's values at 760 $[J \cdot m^{-2} \cdot (4\ day)^{-1}]_{DNA}$ for "first incidence of lesions and retardation of growth in anchovy" and at 1150 $[J \cdot m^{-2} \cdot (4\ day)^{-1}]_{DNA}$ for the "LD_{50} for anchovy" are noted as solid horizontal lines. Figure 11 allows the depth to which these adverse effects occur to be estimated for our different water types and for three ozone thicknesses. For example, if $\omega_{oz} = 0.16$ cm (50% reduction in ozone) the LD_{50} dose would be exceeded at depths above

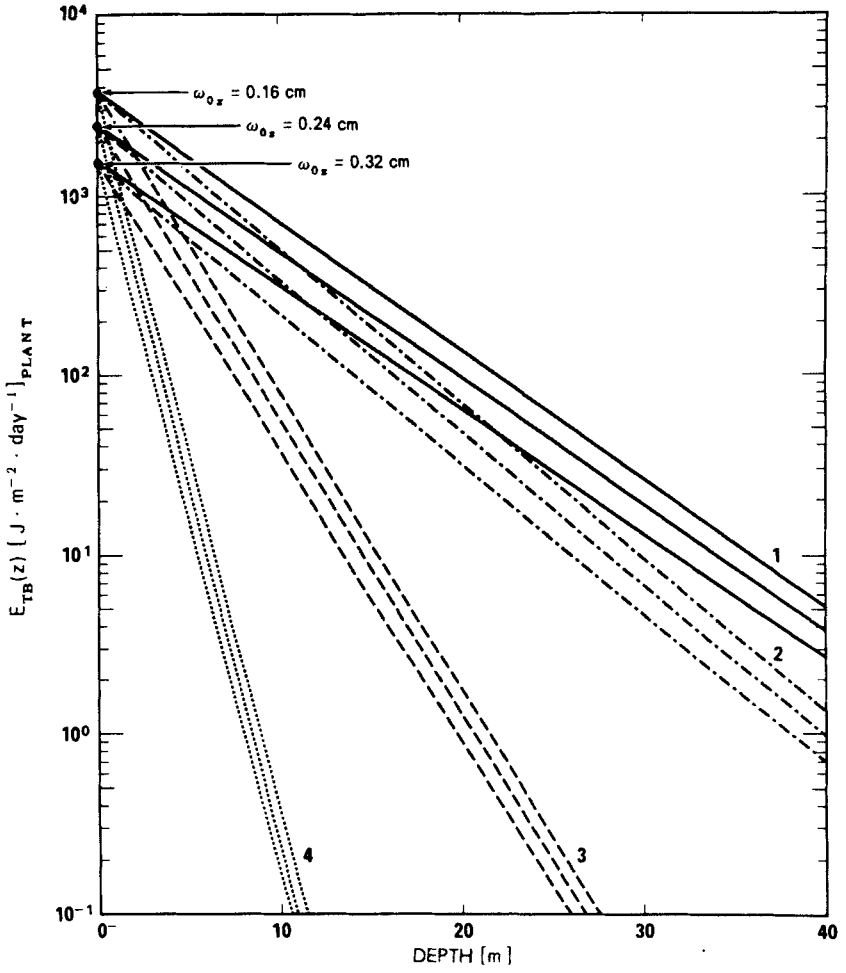

Figure 10. Total daily dose, $E_{TB}(Z)$ $[J \cdot m^{-2} \cdot day^{-1}]_{plant}$ (Caldwell's 1971 generalized plant response action spectrum weighted), vs depth [m]. Notation is the same as for Fig. 9.

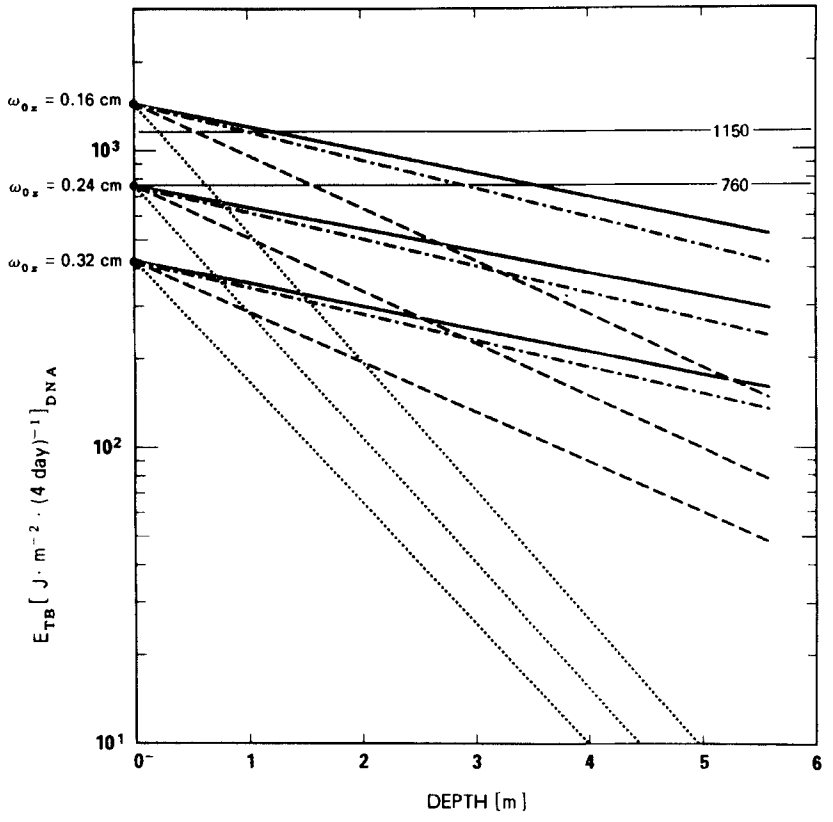

Figure 11. Total 4-day dose, $E_{TB}(Z)$ [J·m^{-2}·(4 day)$^{-1}$]$_{DNA}$ (Setlow DNA action spectrum weighted), vs depth [m]. Notation is the same as for Fig. 9. The horizontal line at 1150 [J·m^{-2}·(4 day)$^{-1}$] indicates Hunter's 4-day LD_{50} dose for anchovy. The line at 760 [J·m^{-2}·(4 day)$^{-1}$] indicates the 4-day "first incidence of lesions and retardation of growth in anchovy" dose (see text for details).

1.2 m in the clearest water, above 0.6 m for the moderately productive waters and above 0.2 m for the water with a high DOM concentration. Under these same conditions, the depths to which the "first lesions" would occur would be 3.5, 1.6, and 0.6 m, respectively. Similarly for ω_{oz} = 0.24 (25% reduction in ozone), the LD_{50} dose would never be exceeded and the "first lesions" would only occur right at the surface.

There is uncertainty, along with natural fluctuations, in the value of the incident total daily UV-B irradiance and hence in $E_{TB}(0^-)$. We have used Green's analytic equations to calculate $E_{TB}(0^+)$, but a change in $E_{TB}(0^+)$ will cause a change in the total biologically effective doses at depth. Since we have shown that there exists an effective attenuation coefficient for irradiance weighted by the Setlow DNA action spectrum, K_{DNA}, a complete spectral calculation at every depth can be replaced by the simpler calculation

$$E_{TB}(Z) = E_{TB}(0^-)e^{-K_{DNA}\cdot Z} \qquad (7)$$

Then graphically, a change in $E_{TB}(0^-)$, for our four water types on Fig. 11, causes a vertical shift between the $E_{TB}(0^-)$ and the horizontal lines representing the results of Hunter *et al.* (1978). Visualizing such a shift graphically demonstrates how changes in $E_{TB}(0^-)$ are translated into changes in the depths to which significant biological effects occur.

It should be emphasized that the horizontal lines in Fig. 11 apply only to our specific example of anchovy. Other aquatic organisms may be more or less sensitive. However, if dosage-response results in units of [J·m^{-2}]$_{DNA}$ for other aquatic organisms can be determined, then their sensitivity to solar UV-B at various depths can also be quantitatively evaluated.

SUMMARY AND DISCUSSION OF ERROR

The few data obtained to date with the underwater UV-spectroradiometer have been used to quantitatively determine the attenuation of UV radiation in various natural water types. Further analysis in terms of biologically effective dose-rates has led to the following conclusions: that a proportional increase of UV radiation (or dose) at the surface results in an approximately similar proportional increase in UV radiation (or dose) at all depths; that the penetration of biologically effective radiation is dependent upon what one defines as "biologically effective" [i.e. on the choice of the weighting function $\epsilon(\lambda)$]; that when the Setlow DNA action spectrum is chosen for $\epsilon(\lambda)$, the spectral change in the wavelength of peak response is relatively small so that there exists an effective attenuation coefficient for DNA, K_{DNA}, for the various water types (Table 2); and that the effective

DNA attenuation length, K_{DNA}^{-1}, is approx. 6 m in the clearest ocean waters and about 2.5 m in moderately productive waters containing average amounts of DOM. In addition, in order to demonstrate how these data can be used to quantitatively evaluate biologically effective dose-rates vs depth, the depths to which detrimental effects of UV radiation on eggs and larvae of the northern anchovy, as determined by Hunter *et al.* (1978), have been calculated for various water types and ozone thicknesses.

The above conclusions are based upon the $K(\lambda)$ data shown in Fig. 1, the use of Green's semi-empirical analytical formulae and the choice of biological weighting function. It is important to keep in mind the particular choice of $\epsilon(\lambda)$ especially when these weighting functions are changing by an order of magnitude every few nanometers near their cutoff edges. As a consequence of the sharp and opposing cutoff edges in the two quantities comprising the integrated response (Fig. 2), only a slight shift in the cutoff edge of either can cause an appreciable change in the integrated response.

Underwater estimates of irradiance levels are subject to the same uncertainties as the input surface values. Thus, any error in $E(0^+,\theta,\lambda)$ from Green's semi-empirical analytic formulae is proportionally propagated to depth.

In addition, the underwater data are subject to uncertainties due to any error in the $K(\lambda)$ data. We estimate our error for the $K(\lambda)$ values given in Table 1 to be less than 15%. This error estimate of 15% applies to the actual data from 310 to 400 nm. As already discussed, $K(\lambda)$ values below 310 nm are based upon a best estimate extrapolation of the actual data. The only justification for this 30 nm extrapolation is that, at present, there is no other more reliable way to obtain $K(\lambda)$ values for this spectral region (Smith and Tyler, 1976). Until new data are available, we will assume that the extrapolated data are a best estimate and that this estimate is not in error more than about 30–50%.

The $K(\lambda)$ values for the clearest ocean water and our data from 22 October 1977 [$K(1)$ and $K(2)$ in Table 1] differ by roughly 20%, due to differences in the Chl concentration. Ignoring (for this discussion of error propagation) this Chl difference, curves $K(1)$ and $K(2)$ may be imagined as two measurements of the same water in error by 20%. Then, a comparison of results based upon these two $K(\lambda)$ curves gives an indication of how a 20% error in $K(\lambda)$ would be propagated through the ensuing calculations to obtain total daily weighted doses vs depth (e.g. Figs. 9, 10 and 11).

Acknowledgements—The design and fabriciation of the underwater UV-spectroradiometer was a Visibility Laboratory team effort. The instrument could not have been completed within the time necessary to meet our cruise schedule without the concerted work of R. W. Austin, J. D. Bailey, G. D. Edwards, R. L. Ensminger, H. G. Sprink and W. H. Wilson. Austin, A. L. Chapin, Edwards and Wilson also helped with the collection of data at sea.

REFERENCES

Austin, R. W. (1974) SIO Ref. 74–10: 2.1–2.20.
Baird, I. (1973) In *Data Rep. Discoverer Expedition* (Edited by J. E. Tyler) Scripps Inst. Oceanogr. Ref. 73–16: C1-C25.
Caldwell, M. M. (1971) In *Photophysiology* (Edited by A. C. Giese) Vol. 6, pp. 131–177, Academic Press, New York.
Calkins, J. (1975) CIAP Monograph 5, Part 1, App. E.
Green, A. E. S., T. Sawada and E. P. Shettle (1974a) *Photochem. Photobiol.* **19**, 251–259.
Green, A. E. S., T. Mo and J. H. Miller (1974b) *Photochem. Photobiol.* **20**, 473–482.
Green, A. E. S. and J. H. Miller (1975) CIAP Monograph 5, Part 1, Chapt. 2.2.4.
Hunter, J. R., J. H. Taylor and H. G. Moser (1978) *Photochem. Phobobiol.* **29**, 325–338.
Jerlov, N. G. (1950) *Nature* 166, 111.
Jerlov, N. G. (1976) *Marine Optics*. Elsevier, New York.
Lenoble, J. (1955) *Compt. Rend.* **241**, 1407–1410.
Lenoble, J. (1956a) *Rev. Opt.* **35**, 526–531.
Lenoble, J. (1956b) *Compt. Rend.* **242**, 806–808.
Lenoble, J. (1956c) *Ann. Geophys.* **12**, 16–31.
Nachtwey, D. S. (1975) CIAP Monograph 5, Part 1, Chapt. 3.
Preisendorfer, R. W. (1976) *Hydrological Optics* Vol. VI, U.S. Dept of Commerce.
Setlow, R. B. (1974) *Proc. Natl. Acad. Sci. U.S.* **71**, 9, 3363–3366.
Shettle, E. P. and A. E. S. Green (1974) *App. Optics* **13**, 1567–1581.
Smith, R. C. and J. E. Tyler (1976) In *Photochemical and Photobiological Reviews* (Edited by K. C. Smith) Vol. 1, pp. 117–155. Plenum Pub. Co., New York.
Smith, R. C. and K. S. Baker (1978a) *Limnol. Oceanogr.* **23**, 247–259.
Smith, R. C. and K. S. Baker (1978b) *Limnol. Oceanogr.* **23**, 260–267.
Stuemer, D. H. (1975) PhD Thesis, Mass. Inst. of Tech.
Tyler, J. E. and R. W. Preisendorfer (1962) In *The Sea* (Edited by M. N. Hill) Vol. 1, 397–451, Interscience, New York.
Tyler, J. E. and R. C. Smith (1966) *J. Opt. Soc. Am.* **56**, 1390–1396.
Tyler, J. E. and R. C. Smith (1970) *Measurements of Spectral Irradiance Underwater*. Gordon & Breach, New York.
Zaneveld, J. R. V. (1975) CIAP Monograph 5, Part 1, Chapt. 2.4.